



OPEN ACCESS

EDITED BY
Yuxing Li,
Xi'an University of Technology, China

REVIEWED BY
Dezhou Kong,
Shandong Agricultural University, China
Ge Tian,
Xi'an University of Technology, China

*CORRESPONDENCE
Kaiping Liu,
kaipiliu@163.com

SPECIALTY SECTION
This article was submitted to Physical
Acoustics and Ultrasonics,
a section of the journal
Frontiers in Physics

RECEIVED 25 September 2022
ACCEPTED 02 November 2022
PUBLISHED 02 December 2022

CITATION
Huang P and Liu K (2022), A new
conjugate gradient algorithm for noise
reduction in signal processing and
image restoration.
Front. Phys. 10:1053353.
doi: 10.3389/fphy.2022.1053353

COPYRIGHT
© 2022 Huang and Liu. This is an open-
access article distributed under the
terms of the [Creative Commons
Attribution License \(CC BY\)](#). The use,
distribution or reproduction in other
forums is permitted, provided the
original author(s) and the copyright
owner(s) are credited and that the
original publication in this journal is
cited, in accordance with accepted
academic practice. No use, distribution
or reproduction is permitted which does
not comply with these terms.

A new conjugate gradient algorithm for noise reduction in signal processing and image restoration

Pan Huang¹ and Kaiping Liu^{2*}

¹School of Mathematics and Information Science, Weifang University, Weifang, Shandong, China,
²School of Management Science, Qufu Normal University, Rizhao, Shandong, China

Noise-reduction methods are an area of intensive research in signal processing. In this article, a new conjugate gradient method is proposed for noise reduction in signal processing and image restoration. The superiority of this method lies in its employment of the ideas of accelerated conjugate gradient methods in conjunction with a new adaptive method for choosing the step size. In this work, using some assumptions, the weak convergence of the designed method was established. As example applications, we implemented our method to solve signal-processing and image-restoration problems. The results of our numerical simulations demonstrate the effectiveness and superiority of the new approach.

KEYWORDS

signal processing, image restoration, weak convergence, noise reduction, conjugate gradient method

1 Introduction

Noise reduction is an important step in signal pre-processing; it is widely applied in many fields, including underwater acoustic imaging [1, 2], pattern recognition [3], and target detection and feature extraction [4], among others [5]. In this article, a new approach based on a conjugate gradient method is derived from mathematical principles.

We consider the degradation model of signal or image such as:

$$y = \mathcal{A}\omega + \varepsilon, \quad (1)$$

where $\omega \in \mathbb{R}^N$ is an original signal or image, \mathcal{A} is the degradation operator, ε is the noise, $y \in \mathbb{R}^M$ is the observed data. The essence of noise reduction is solving Eq. 1 to obtain ω . The solving of Eq. 1 can be considered as the following problem [6]:

$$\min_{\omega \in \mathbb{R}^N} \frac{1}{2} \|y - \mathcal{A}\omega\|^2 \text{ s.t. } \|\omega\|_1 \leq r, \quad (2)$$

where $r > 0$ and $\|\cdot\|_1$ is the ℓ_1 norm. Let $C = \{\omega \in \mathbb{R}^N: \|\omega\|_1 \leq r\}$ and $Q = \{y\}$, then Eq. 2 can be seen as a split feasibility problem (SFP) [7–10]. Thus, we translate the problem of noise reduction to SFP, which can be described as:

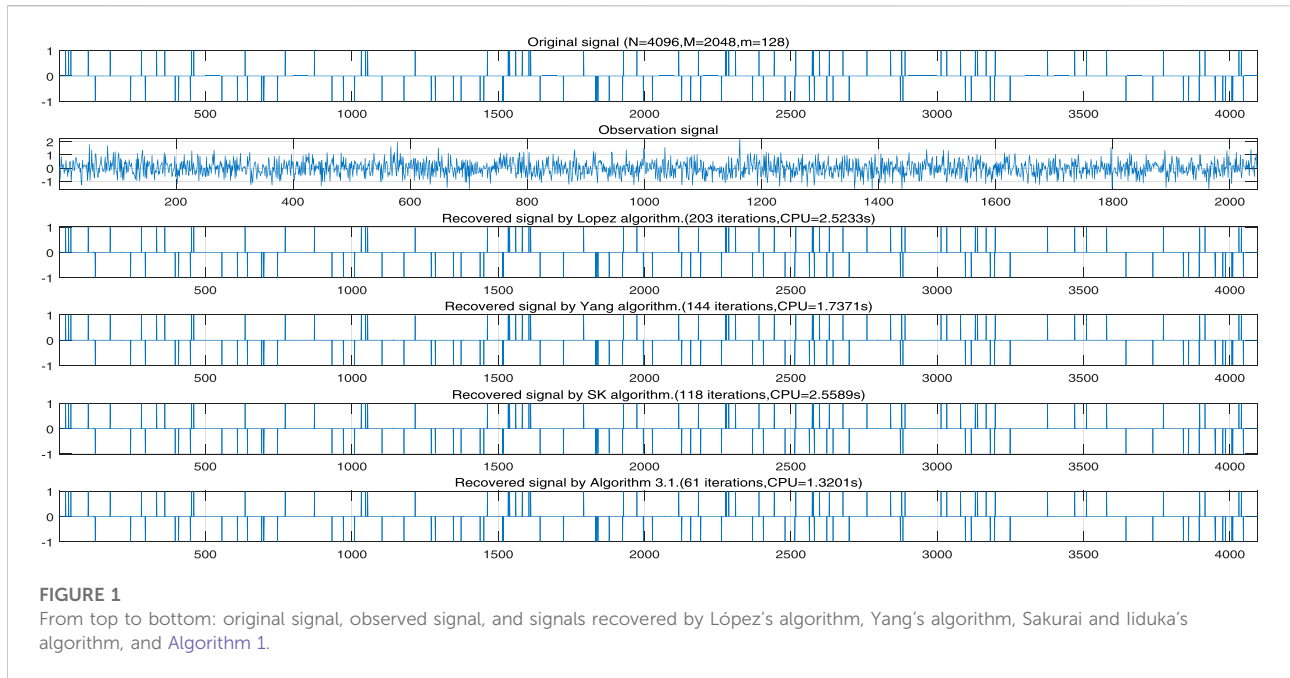


FIGURE 1 From top to bottom: original signal, observed signal, and signals recovered by López’s algorithm, Yang’s algorithm, Sakurai and liduka’s algorithm, and Algorithm 1.

$$\text{find } \omega \in C \text{ such that } \mathcal{A}\omega \in Q, \tag{3}$$

where H_1 and H_2 are real Hilbert spaces, $\mathcal{A}: H_1 \rightarrow H_2$ is a bounded linear operator, the closed and convex set $C \subset H_1$ ($C \neq \emptyset$), and $Q \subset H_2$ ($Q \neq \emptyset$). In order to solve the SFP, Byrne [11, 12] presented the CQ algorithm, which creates a sequence $\{\omega_i\}$:

$$\omega_{i+1} = P_C(\omega_i - \tau_i \mathcal{A}^*(I - P_Q)\mathcal{A}\omega_i), \tag{4}$$

where P_C is the projection to C , P_Q is the projection to Q , $\tau_i \in (0, \frac{2}{\|\mathcal{A}\|^2})$, and \mathcal{A}^* is the adjoint operator of \mathcal{A} . For convex functions c and q , the definitions of C and Q are

$$C = \{\omega \in H_1: c(\omega) \leq 0\} \text{ and } Q = \{u \in H_2: q(u) \leq 0\}.$$

There have been some research works devoted to solving Eq. 3. In 2004, Yang [13] presented a relaxed CQ algorithm using P_C and P_Q to replace P_C and P_Q . Here, we define two sets at point ω_i by

$$C_i = \{\omega \in H_1: c(\omega_i) \leq \langle \zeta_i, \omega_i - \omega \rangle\}, \tag{5}$$

where $\zeta_i \in \partial c(\omega_i)$, and

$$Q_i = \{u \in H_2: q(\mathcal{A}\omega_i) \leq \langle \vartheta_i, \mathcal{A}\omega_i - u \rangle\}, \tag{6}$$

where $\vartheta_i \in \partial q(\mathcal{A}\omega_i)$. For all $i > 1$, clearly, $C \subseteq C_i$ and $Q \subseteq Q_i$. In addition, C_i and Q_i are half-spaces. Furthermore, referring to [14], we define

$$f_i(\omega) = \frac{1}{2} \|(I - P_{C_i})\omega\|^2 + \frac{1}{2} \|(I - P_{Q_i})\mathcal{A}\omega\|^2, \tag{7}$$

where C_i and Q_i are given as in Eqs. 5, 6. In this specific case, their gradient is

$$\nabla f_i(\omega) = (I - P_{C_i})\omega + \mathcal{A}^*(I - P_{Q_i})\mathcal{A}\omega. \tag{8}$$

Yang [13] presented a relaxed CQ algorithm in a finite-dimensional Hilbert space:

$$\omega_{i+1} = P_C(\omega_i - \tau_i \nabla f_i(\omega_i)), \tag{9}$$

where $\tau_i \in (0, \frac{2}{\|\mathcal{A}\|^2})$. Notice that calculating $\|\mathcal{A}\|$ is complex and costly when \mathcal{A} is a high-dimensional dense matrix. In 2005, Yang [15] presented a new adaptive step size τ_i , which is defined as:

$$\tau_i = \frac{\rho_i}{\|\nabla f_i(x_i)\|}, \tag{10}$$

where

$$\sum_{i=1}^{\infty} \rho_i = \infty, \quad \sum_{i=1}^{\infty} \rho_i^2 < +\infty.$$

However, Yang’s step size (Eq. 10) requires that Q_i is bounded and the matrix \mathcal{A} is full rank. Recently, Wang [16] absolutely eliminated these problems. Considering the CQ algorithm, López [17] introduced a novel step size to overcome these problems; this is defined as:

$$\tau_i = \frac{\rho_i f_i(x_i)}{\|\nabla f_i(x_i)\|^2}, \tag{11}$$

where $\rho_i \in (0, 4)$. With López’s step size (Eq. 11), it was proved that $\{\omega_i\}$ in Eq. 9 weakly converges to the solution of the SFP.

In 2005, Qu and Xiu [18] introduced a relaxed CQ algorithm that is improved by using an Armijo line search in Euclidian space. In 2017, on the basis of the above application, Gibali [19] extended this to Hilbert spaces, which proved that $\{\omega_i\}$ weakly converges to a solution of the SFP as follows:

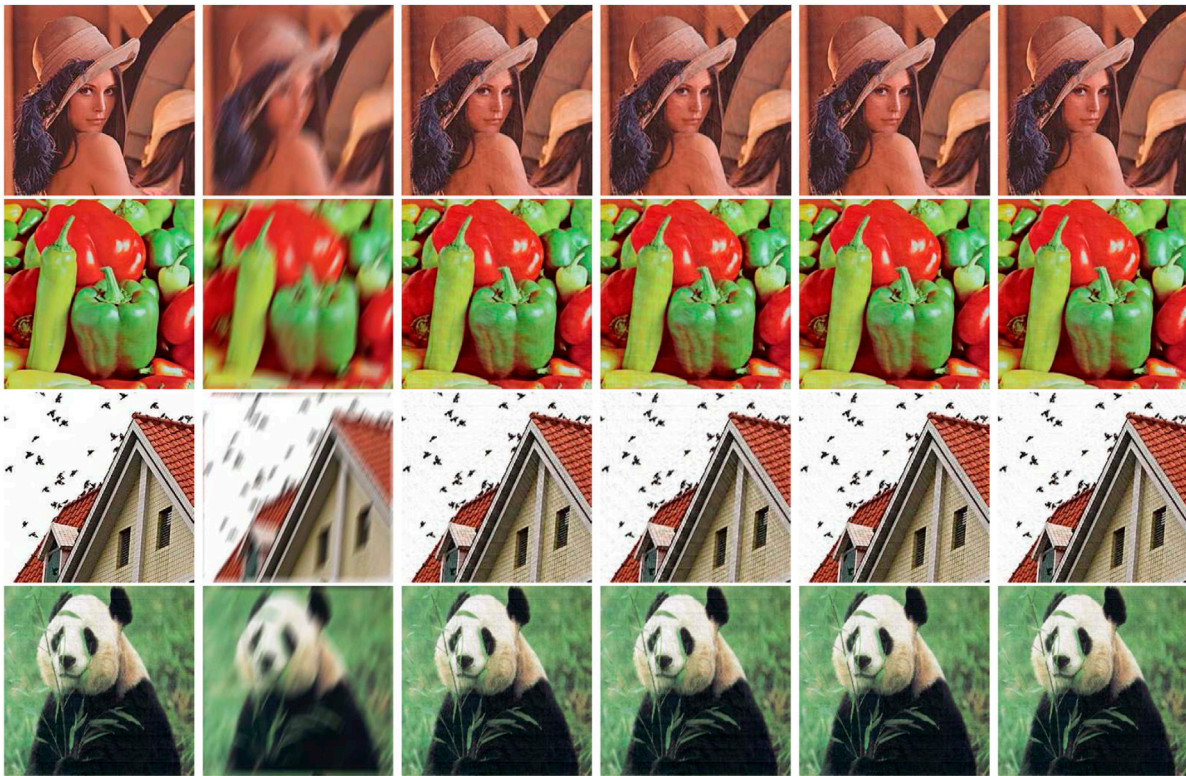


FIGURE 2 Comparison of recovered color images of Lena, peppers, house, panda using different algorithms with 1,000 iterations. From left to right: original image, noised image, López's algorithm, Yang's algorithm, Sakurai and Iiduka's algorithm, and Algorithm 1.

$$\begin{aligned} y_i &= P_{C_i}(\omega_i - \tau_i \nabla f_i(\omega_i)), \\ \omega_{i+1} &= P_{C_i}(\omega_i - \tau_i \nabla f_i(y_i)), \end{aligned} \tag{12}$$

where $\tau_i = \gamma \ell^i$, $\gamma > 0$, $\ell \in (0, 1)$, i is the smallest nonnegative integer, and $\nu \in (0, 1)$ satisfies:

$$\tau_i \|\nabla f_i(\omega_i) - \nabla f_i(y_i)\| \leq \nu \|\omega_i - y_i\|.$$

In 2020, Kesornprom et al. [20] introduced a gradient-CQ algorithm that derived a weak-convergence theorem for solving the SFP in the framework of Hilbert spaces. This is described as:

$$\begin{aligned} y_i &= \omega_i - \tau_i \nabla f_i(\omega_i), \\ \omega_{i+1} &= P_{C_i}(y_i - \varphi_i \nabla f_i(y_i)), \end{aligned}$$

where C_i , f_i , and ∇f_i are given in Eqs 5, 7, 8, respectively, and

$$\begin{aligned} \tau_i &= \frac{\rho_i f_i(\omega_i)}{\|\nabla f_i(\omega_i)\|^2 + \theta_i}, \text{ and} \\ \varphi_i &= \frac{\rho_i f_i(y_i)}{\|\nabla f_i(y_i)\|^2 + \theta_i}, \quad 0 < \rho_i < 4, \quad 0 < \theta_i < 1. \end{aligned}$$

The conjugate gradient method [21] is a commonly used acceleration scheme in the steepest descent method. The conjugate gradient direction of f at ω_i is

$$d_{i+1} = -\nabla f_i(\omega_i) + \beta_i d_i,$$

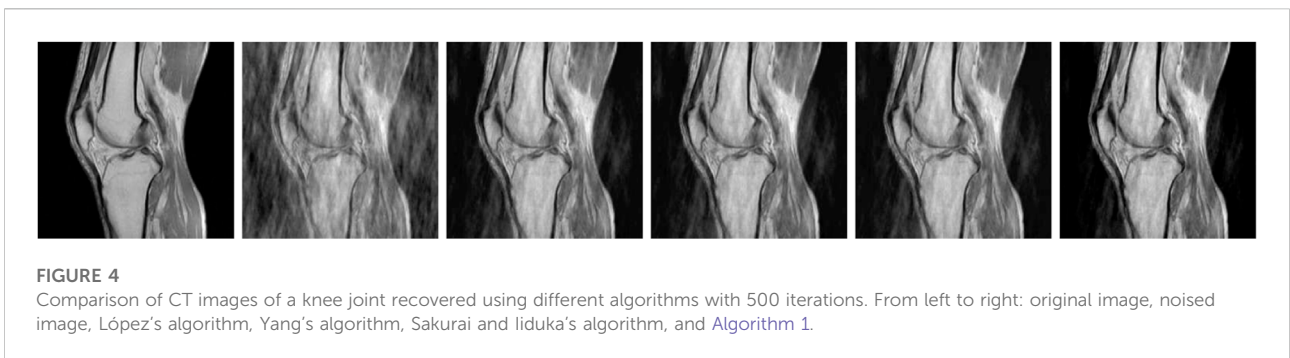
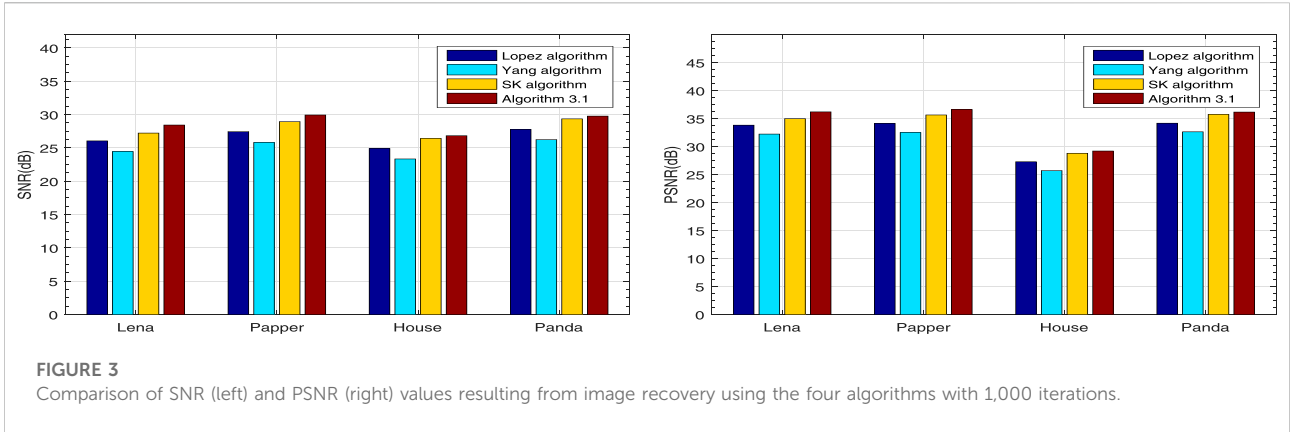
where $d_0 = -\nabla f(\omega_0)$ and $\beta_i \in (0, \infty)$. In this article, motivated by previous works [22–24], a new viscosity approximation method based on the conjugate gradient method is introduced. Many other iterative methods of solving the SFP have been proposed [25–29].

Herein, combining the relaxed CQ algorithm with a new step size and the conjugate gradient method, we find the solution of noise reduction problem in Eq. 1 by solving the SFP in Hilbert spaces with a novel approach. Section 2 gives some basic definitions and lemmas. In Section 3, the theorem for proving the weak convergence of our method is presented. In Section 4, we present experimental results and compare them with the relaxed CQ algorithms of López [17], Yang [15], and Sakurai and Iiduka [20]. Finally, conclusions are given in Section 5.

2 Preliminaries

Throughout this article, to obtain our results, some technical lemmas are used.

Lemma 2.1 [30]. *Suppose the nonempty set $C \subset H_1$ is closed and convex. Thus, for all $h_1, h_2 \in H_1$ and $c \in C$,*



- (i) $\langle h_1 - P_C h_1, c - P_C h_1 \rangle \leq 0$;
- (ii) $\|P_C h_1 - P_C h_2\|^2 \leq \langle P_C h_1 - P_C h_2, h_1 - h_2 \rangle$;
- (iii) $\|P_C h_1 - c\|^2 \leq \|h_1 - c\|^2 - \|P_C h_1 - h_1\|^2$.

From Lemma 2.1(ii), let I express the identity operator; then, $I - P_C$ is a firmly nonexpansive operator, i.e.,

$$\|(I - P_C)h_1 - (I - P_C)h_2\|^2 \leq \langle (I - P_C)h_1 - (I - P_C)h_2, h_1 - h_2 \rangle, \forall h_1, h_2 \in H_1.$$

Definition 1. Suppose \mathbb{R} is a set of real numbers, $G: H \rightarrow \mathbb{R}$ is convex; the definition of its subdifferential at w is then

$$\partial G(w) = \{ \zeta \in H \mid G(z) \geq G(w) + \langle \zeta, z - w \rangle, \forall z \in H \}.$$

To obtain our results, we prove the following lemma.

Lemma 2.2. Let $f_i(w)$ be defined in Eq. 7; then ∇f_i is Lipschitz continuous with Lipschitz constant $1 + \|\mathcal{A}\|^2$

Proof. For any $p, q \in H$,

$$\begin{aligned} \|\nabla f_i(p) - \nabla f_i(q)\| &= \|(I - P_C)p - (I - P_C)q + \mathcal{A}^*(I - P_Q)\mathcal{A}p - \mathcal{A}^*(I - P_Q)\mathcal{A}q\| \\ &\leq \|p - P_C p + P_C q - q\| + \|\mathcal{A}^*(I - P_Q)\mathcal{A}p - \mathcal{A}^*(I - P_Q)\mathcal{A}q\| \\ &\leq \|p - q\| + \|\mathcal{A}\| \|(I - P_Q)\mathcal{A}p - (I - P_Q)\mathcal{A}q\| \\ &\leq \|p - q\| + \|\mathcal{A}\| \|\mathcal{A}p - \mathcal{A}q\| \\ &\leq \|p - q\| + \|\mathcal{A}\|^2 \|p - q\| \\ &= (1 + \|\mathcal{A}\|^2) \|p - q\|. \end{aligned}$$

So, ∇f_i is $1 + \|\mathcal{A}\|^2$ -Lipschitz continuous.

3 Algorithm and convergence

A novel gradient-CQ algorithm is established in this section. Furthermore, we prove that the sequence created by our approach is convergent.

Algorithm 1. Let $\alpha_1, \alpha_2, \beta_i, \hat{\beta}_i \in (0, 1)$, and the sequences $\{d_i\}, \{\omega_i\}, \{y_i\}, \{\hat{d}_i\}$, and $\{z_i\}$ be denoted as:

$$\begin{aligned} d_{i+1} &= -\tau_i \nabla f_i(\omega_i) + \alpha_1 \beta_i d_i, \\ y_i &= \omega_i + d_{i+1}, \\ \hat{d}_{i+1} &= -\varphi_i \nabla f_i(y_i) + \alpha_2 \hat{\beta}_i \hat{d}_i, \\ z_i &= y_i + \hat{d}_{i+1}, \\ \omega_{i+1} &= P_{C_i}(z_i), \end{aligned}$$

where $\tau_i = \frac{\rho_i f_i(\omega_i)}{\|\nabla f_i(\omega_i)\|^2 + \theta_i}$, $\varphi_i = \frac{\rho_i f_i(y_i)}{\|\nabla f_i(y_i)\|^2 + \theta_i}$, and $0 < \rho_i < 4, 0 < \theta_i < 1$.

We next state our weak-convergence theorem.

Theorem 3.1. The following assumptions hold:

- (C1) $\inf_i \rho_i (4 - \rho_i) > 0$;
- (C2) $\lim_{i \rightarrow \infty} \theta_i = 0$;
- (C3) $\lim_{i \rightarrow \infty} \beta_i = 0, \lim_{i \rightarrow \infty} \hat{\beta}_i = 0$
- (C4) $\{(I - P_{C_i})\omega_i\}_{i \rightarrow \infty}$ and $\{(I - P_{Q_i})\mathcal{A}\omega_i\}$ are bounded.

So, $\{\omega_i\}$ in Algorithm 1 converges weakly to $\omega^* \in \Omega$, which is the nonempty solution set of the SFP.

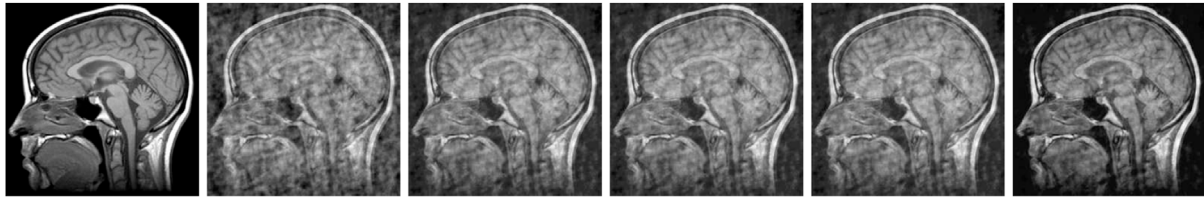


FIGURE 5
Comparison of CT images of a head recovered using different algorithms with 500 iterations. From left to right: original image, noised image, López's algorithm, Yang's algorithm, Sakurai and Iiduka's algorithm, and Algorithm 1.

Proof. First, by using mathematical induction, we show that $\{d_i\}$ and $\{\hat{d}_i\}$ are bounded. Assume that $\|d_i\| \leq M$ holds, for some $i \geq i_0$. Assumption C3 implies that there exists $i_0 \in \mathbb{N}$ such that $\beta_i \leq \frac{1}{2}, \forall i \geq i_0$. Let $M = \max\{\|d_{i_0}\|, 2 \sup_{i \geq 1} \|\tau_i [(I - P_{C_i})\omega_i + \mathcal{A}^*(I - P_{Q_i})\mathcal{A}\omega_i]\|\} < \infty$. From Algorithm 1, the triangle inequality guarantees that

$$\begin{aligned} \|d_{i+1}\| &= \|\tau_i [(I - P_{C_i})\omega_i + \mathcal{A}^*(I - P_{Q_i})\mathcal{A}\omega_i] + \alpha_i \beta_i d_i\| \\ &\leq \|\tau_i [(I - P_{C_i})\omega_i + \mathcal{A}^*(I - P_{Q_i})\mathcal{A}\omega_i]\| + \alpha_i \beta_i \|d_i\| \\ &\leq M, \end{aligned}$$

which means that $\|d_i\| \leq M$ for all $i \geq i_0$, so $\{d_i\}$ is bounded.

Assume that $\|\hat{d}_i\| \leq \hat{M}$ is true for some $i \geq i_0$ and let $\hat{M} = \max\{\|\hat{d}_{i_0}\|, 2 \sup_{i \geq 1} \|\varphi_i [(I - P_{C_i})x_i + \mathcal{A}^*(I - P_{Q_i})\mathcal{A}x_i]\|\} < \infty$. As with the proof that $\|d_i\|$ is bounded, we deduce

$$\begin{aligned} \|\hat{d}_{i+1}\| &= \|\varphi_i [(I - P_{C_i})y_i + \mathcal{A}^*(I - P_{Q_i})\mathcal{A}y_i] + \alpha_2 \hat{\beta}_i \hat{d}_i\| \\ &\leq \|\varphi_i [(I - P_{C_i})y_i + \mathcal{A}^*(I - P_{Q_i})\mathcal{A}y_i]\| + \alpha_2 \hat{\beta}_i \|\hat{d}_i\| \\ &\leq \hat{M}. \end{aligned}$$

Let $z \in \Omega$. Since $Q \subseteq Q_i$ and $C \subseteq C_i$, we obtain $Az = P_{Q_i}(Az) = P_Q(Az)$ and $z = P_{C_i}(z) = P_C(z)$. We have $\nabla f_i(z) = 0$. From Lemma 2.1(iii),

$$\begin{aligned} \|\omega_{i+1} - z\|^2 &= \|P_{C_i}(z_i) - z\|^2 \\ &\leq \|z_i - z\|^2 - \|P_{C_i}(z_i) - z_i\|^2 \\ &= \|z_i - z\|^2 - \|\omega_{i+1} - z_i\|^2. \end{aligned} \tag{13}$$

Combining Lemma 2.1(ii), Eq. 7, and Eq. 8, we obtain

$$\begin{aligned} \langle \nabla f_i(y_i), y_i - z \rangle &= \langle (I - P_{C_i})y_i, y_i - z \rangle + \langle \mathcal{A}^*(I - P_{Q_i})\mathcal{A}y_i, y_i - z \rangle \\ &= \langle (I - P_{C_i})y_i, y_i - z \rangle + \langle (I - P_{Q_i})\mathcal{A}y_i, \mathcal{A}y_i - \mathcal{A}z \rangle \\ &\geq \|(I - P_{C_i})y_i\|^2 + \|(I - P_{Q_i})\mathcal{A}y_i\|^2 \\ &= 2f_i(y_i). \end{aligned} \tag{14}$$

as with Eq. 14, it follows that

$$\langle \nabla f_i(\omega_i), \omega_i - z \rangle \geq 2f_i(\omega_i).$$

notice that

$$\begin{aligned} \|y_i - z - \varphi_i \nabla f_i(y_i)\|^2 &= \|y_i - z\|^2 + \varphi_i^2 \|\nabla f_i(y_i)\|^2 - 2\varphi_i \langle \nabla f_i(y_i), y_i - z \rangle \\ &\leq \|y_i - z\|^2 + \varphi_i^2 \|\nabla f_i(y_i)\|^2 - 4\varphi_i f_i(y_i) \\ &= \|y_i - z\|^2 + \rho_i^2 \frac{f_i^2(y_i)}{(\|\nabla f_i(y_i)\|^2 + \theta_i)^2} \|\nabla f_i(y_i)\|^2 \\ &\quad - 4\rho_i \frac{f_i^2(y_i)}{\|\nabla f_i(y_i)\|^2 + \theta_i} \\ &\leq \|y_i - z\|^2 + \rho_i^2 \frac{f_i^2(y_i)}{(\|\nabla f_i(y_i)\|^2 + \theta_i)^2} (\|\nabla f_i(y_i)\|^2 + \theta_i) \\ &\quad - 4\rho_i \frac{f_i^2(y_i)}{\|\nabla f_i(y_i)\|^2 + \theta_i} \\ &= \|y_i - z\|^2 - \rho_i(4 - \rho_i) \frac{f_i^2(y_i)}{\|\nabla f_i(y_i)\|^2 + \theta_i}. \end{aligned} \tag{15}$$

similar to Eq. 15, we deduce

$$\begin{aligned} \|\omega_i - z - \tau_i \nabla f_i(\omega_i)\|^2 &= \|\omega_i - z\|^2 + \tau_i^2 \|\nabla f_i(\omega_i)\|^2 - 2\tau_i \langle \nabla f_i(\omega_i), \omega_i - z \rangle \\ &\leq \|\omega_i - z\|^2 + \tau_i^2 \|\nabla f_i(\omega_i)\|^2 - 4\tau_i f_i(\omega_i) \\ &= \|\omega_i - z\|^2 + \rho_i^2 \frac{f_i^2(\omega_i)}{(\|\nabla f_i(\omega_i)\|^2 + \theta_i)^2} \|\nabla f_i(\omega_i)\|^2 \\ &\quad - 4\rho_i \frac{f_i^2(\omega_i)}{\|\nabla f_i(\omega_i)\|^2 + \theta_i} \\ &\leq \|\omega_i - z\|^2 + \rho_i^2 \frac{f_i^2(\omega_i)}{(\|\nabla f_i(\omega_i)\|^2 + \theta_i)^2} (\|\nabla f_i(\omega_i)\|^2 + \theta_i) \\ &\quad - 4\rho_i \frac{f_i^2(\omega_i)}{\|\nabla f_i(\omega_i)\|^2 + \theta_i} \\ &= \|\omega_i - z\|^2 - \rho_i(4 - \rho_i) \frac{f_i^2(\omega_i)}{\|\nabla f_i(\omega_i)\|^2 + \theta_i}. \end{aligned} \tag{16}$$

Furthermore, combining Algorithm 1, and Eq. 15, we have

$$\begin{aligned} \|z_i - z\|^2 &\leq \|y_i - z - \varphi_i \nabla f_i(y_i) + \alpha_2 \hat{\beta}_i \hat{d}_i\|^2 \\ &= \|y_i - z - \varphi_i \nabla f_i(y_i)\|^2 + \|\alpha_2 \hat{\beta}_i \hat{d}_i\|^2 \\ &\quad + 2\langle y_i - z - \varphi_i \nabla f_i(y_i), \alpha_2 \hat{\beta}_i \hat{d}_i \rangle \\ &\leq \|y_i - z - \varphi_i \nabla f_i(y_i)\|^2 \\ &\quad + 2\langle y_i - z - \varphi_i \nabla f_i(y_i) + \alpha_2 \hat{\beta}_i \hat{d}_i, \alpha_2 \hat{\beta}_i \hat{d}_i \rangle \\ &\leq \|y_i - z - \varphi_i \nabla f_i(y_i)\|^2 + 2\alpha_2 \hat{\beta}_i \langle z_i - z, \hat{d}_i \rangle \\ &\leq \|y_i - z\|^2 - \rho_i(4 - \rho_i) \frac{f_i^2(y_i)}{\|\nabla f_i(y_i)\|^2 + \theta_i} + \hat{\beta}_i \hat{M}, \end{aligned} \tag{17}$$

where $\hat{M} = \sup_{i \in \mathbb{N}} 2\alpha_2 \langle z_i - z, \hat{d}_i \rangle$. As with Eq. 17, we deduce

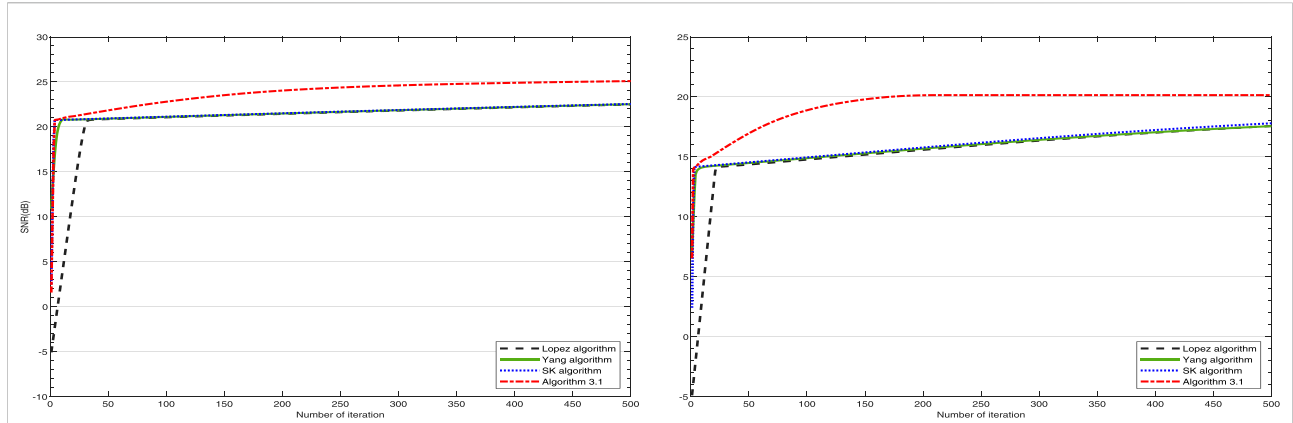


FIGURE 6 Comparison of SNR values of the knee joint (left) and head (right) images resulting from image recovery using the four algorithms with 500 iterations.

$$\begin{aligned} \|y_i - z\|^2 &= \|\omega_i - z - \tau_i \nabla f_i(\omega_i) + \alpha_i \beta_i \hat{d}_i\|^2 \\ &\leq \|\omega_i - z - \tau_i \nabla f_i(\omega_i)\|^2 + 2\alpha_i \beta_i \langle y_i - z, \hat{d}_i \rangle \\ &\leq \|\omega_i - z\|^2 - \rho_i(4 - \rho_i) \frac{f_i^2(\omega_i)}{\|\nabla f_i(\omega_i)\|^2 + \theta_i} + \beta_i M, \end{aligned} \quad (18)$$

where $M = \sup_{i \in N} 2\alpha_i \langle y_i - z, \hat{d}_i \rangle$. Thus, from Eqs 13, 17, 18, it holds that

$$\begin{aligned} \|\omega_{i+1} - z\|^2 &\leq \|y_i - z\|^2 - \rho_i(4 - \rho_i) \frac{f_i^2(y_i)}{\|\nabla f_i(y_i)\|^2 + \theta_i} + \hat{\beta}_i \hat{M} \\ &\quad - \|\omega_{i+1} - y_i + \varphi_i \nabla f_i(y_i) - \alpha_2 \hat{\beta}_i \hat{d}_i\|^2 \\ &\leq \|\omega_i - z\|^2 - \rho_i(4 - \rho_i) \left(\frac{f_i^2(\omega_i)}{\|\nabla f_i(\omega_i)\|^2 + \theta_i} + \frac{f_i^2(y_i)}{\|\nabla f_i(y_i)\|^2 + \theta_i} \right) \\ &\quad + (\beta_i M + \hat{\beta}_i \hat{M}) - \|\omega_{i+1} - y_i + \varphi_i \nabla f_i(y_i) - \alpha_2 \hat{\beta}_i \hat{d}_i\|^2. \end{aligned} \quad (19)$$

from Theorem 3.1(C3) and $0 < \rho_i < 4$, we deduce

$$\|\omega_{i+1} - z\| \leq \|\omega_i - z\|.$$

Therefore, $\lim_{i \rightarrow \infty} \|\omega_i - z\|$ exists; hence $\{\omega_i\}$ is bounded. Consequently, $\{y_i\}$ and $\{z_i\}$ are bounded. Back to the previous step (Eq. 19), we obtain

$$\liminf_{i \rightarrow \infty} \rho_i(4 - \rho_i) \left(\frac{f_i^2(\omega_i)}{\|\nabla f_i(\omega_i)\|^2 + \theta_i} + \frac{f_i^2(y_i)}{\|\nabla f_i(y_i)\|^2 + \theta_i} \right) = 0,$$

which implies by (C2) and (C3) of Theorem 3.1 that

$$\lim_{i \rightarrow \infty} \frac{f_i^2(\omega_i)}{\|\nabla f_i(\omega_i)\|^2} = \lim_{i \rightarrow \infty} \frac{f_i^2(y_i)}{\|\nabla f_i(y_i)\|^2} = 0. \quad (20)$$

furthermore, it yields

$$\begin{aligned} \|\nabla f_i(\omega_i)\| &= \|\nabla f_i(\omega_i) - \nabla f_i(z)\| \leq L\|\omega_i - z\|, \\ \|\nabla f_i(y_i)\| &= \|\nabla f_i(y_i) - \nabla f_i(z)\| \leq L\|y_i - z\|, \end{aligned} \quad (21)$$

where $L = 1 + \|\mathcal{A}\|^2$. This implies that $\|\nabla f_i(\omega_i)\|$ and $\|\nabla f_i(y_i)\|$ are bounded. From Eqs 20, 21, we have

$$\lim_{i \rightarrow \infty} f_i(\omega_i) = \lim_{i \rightarrow \infty} f_i(y_i) = 0,$$

which implies



FIGURE 7 Original image.

$$\begin{aligned} &\lim_{i \rightarrow \infty} (\|(I - P_{C_i})\omega_i\| + \|(I - P_{Q_i})\mathcal{A}\omega_i\|) \\ &= \lim_{i \rightarrow \infty} (\|(I - P_{C_i})y_i\| + \|(I - P_{Q_i})\mathcal{A}y_i\|) = 0. \end{aligned}$$

Moreover, from Eq. 19, we have

$$\lim_{i \rightarrow \infty} \|\omega_{i+1} - y_i + \varphi_i \nabla f_i(y_i) - \alpha_2 \hat{\beta}_i \hat{d}_i\| = 0. \quad (22)$$

We notice that

$$\lim_{i \rightarrow \infty} \varphi_i \|\nabla f_i(y_i)\| = \lim_{i \rightarrow \infty} \left(\frac{\rho_i f_i(y_i)}{\|\nabla f_i(y_i)\|^2 + \theta_i} \|\nabla f_i(y_i)\| \right) = 0. \quad (23)$$

Therefore, combining Eqs. 22, 23 and $\lim_{i \rightarrow \infty} \hat{\beta}_i = 0$, we have

$$\lim_{i \rightarrow \infty} \|\omega_{i+1} - y_i\| = 0.$$

In addition, from Algorithm 1 and Theorem 3.1(C3), we obtain

$$\lim_{i \rightarrow \infty} \|y_i - \omega_i\| = \lim_{i \rightarrow \infty} (\tau_i \|\nabla f_i(\omega_i)\|) = 0.$$

Then, we deduce

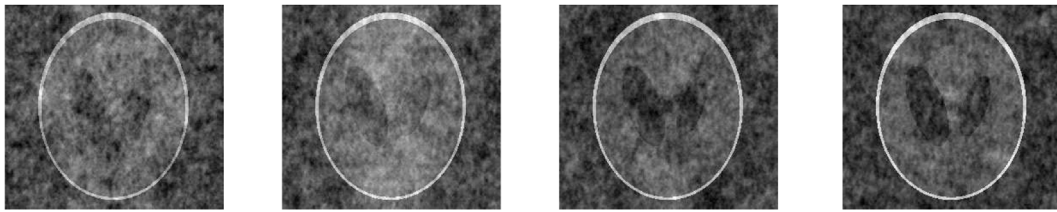


FIGURE 8
Versions of the image in Figure 7 with sampling rates of 30%, 40%, 50%, and 60% from left to right.

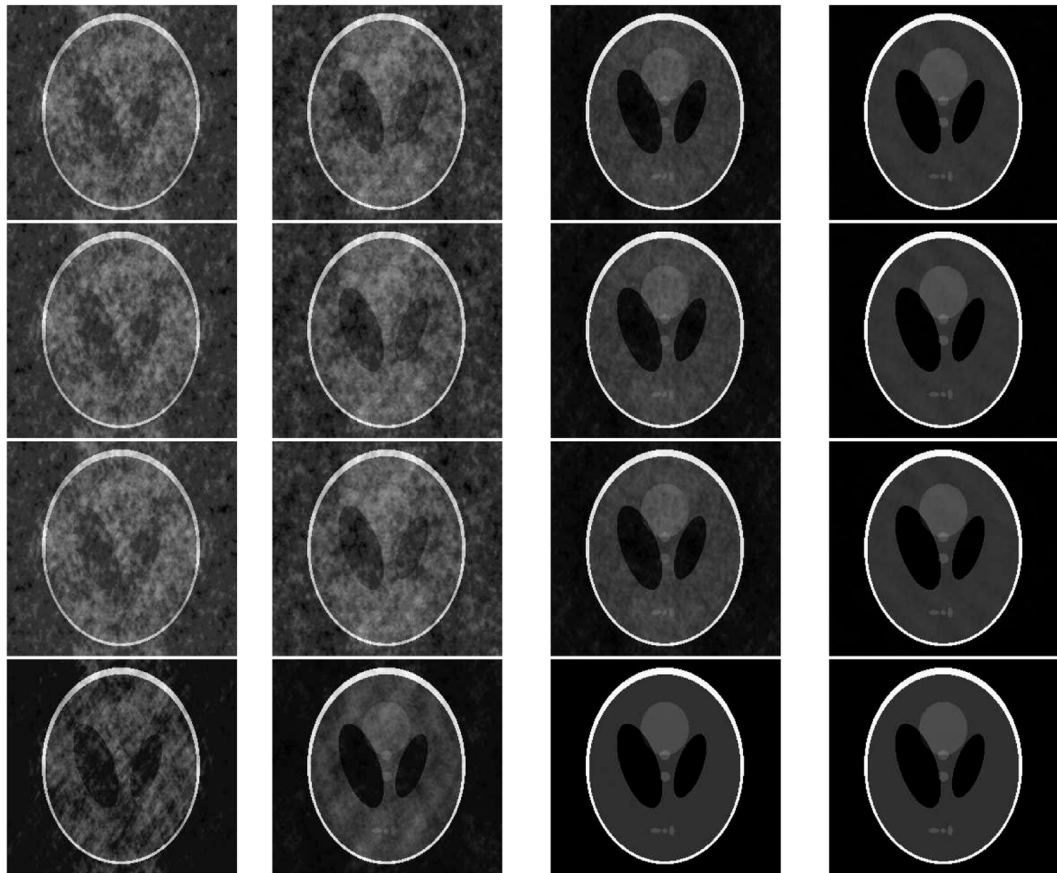


FIGURE 9
Comparison of images recovered using the four algorithms. From top to bottom: López's algorithm, Yang's algorithm, Sakurai and Iiduka's algorithm, and Algorithm 1; from left to right: sampling rates of 30%, 40%, 50%, and 60%.

$$\lim_{i \rightarrow \infty} \|\omega_{i+1} - \omega_i\| = 0,$$

considering $\{\omega_i\}$ is bounded. Consequently, we can find a subsequence $\{\omega_{i_k}\} \rightarrow \omega^*$ and $\omega^* \in H_1$. Subsequently, we prove $\omega^* \in \Omega$. Using Eq. 5, and the fact that $\omega_{k+1} \in C_{i_k}$, we have

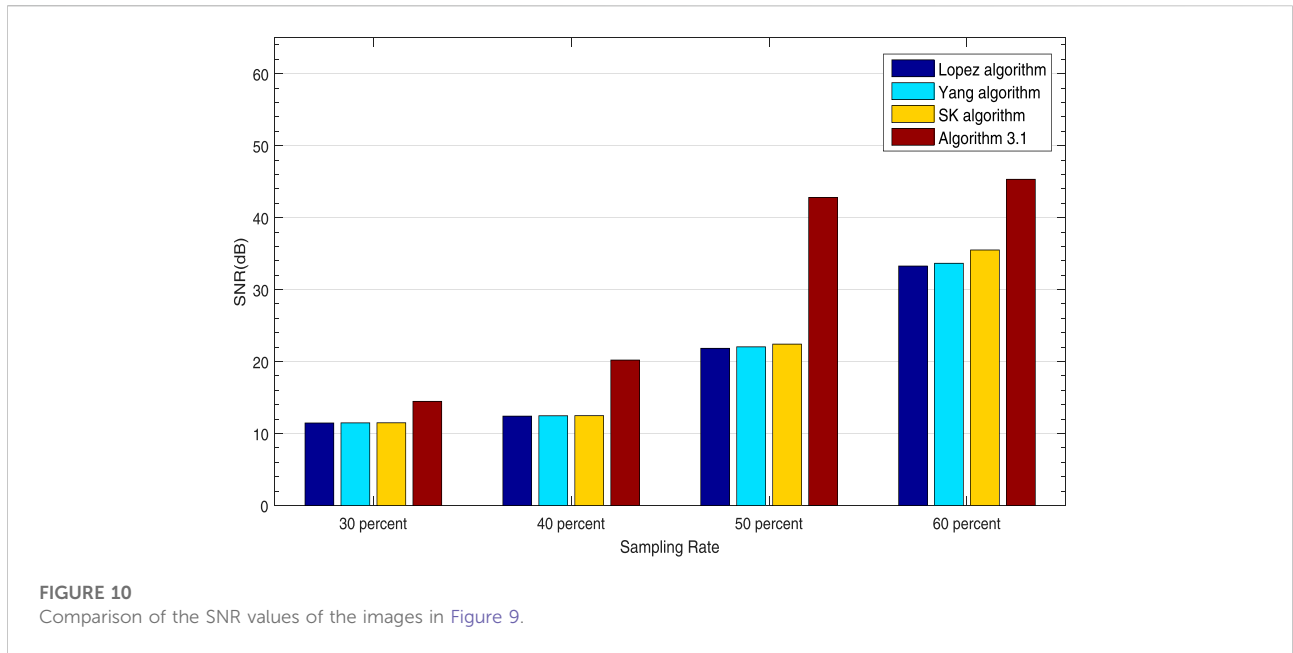
$$c(\omega_{i_k}) \leq \langle \zeta_{i_k}, \omega_{i_k} - \omega_{i_k+1} \rangle,$$

where $\zeta_{i_k} \in \partial c(\omega_{i_k})$. Applying the boundedness of ∂c , it follows that

$$c(\omega_{i_k}) \leq \|\zeta_{i_k}\| \|\omega_{i_k} - \omega_{i_k+1}\| \rightarrow 0, k \rightarrow \infty. \tag{24}$$

From $\omega_{i_k} \rightarrow \omega^*$ and Eq. 24, we deduce

$$c(\omega^*) \leq \liminf_{k \rightarrow \infty} c(\omega_{i_k}) \leq 0.$$



Hence, $\omega^* \in C$. Then, we show that $\mathcal{A}\omega^* \in Q$. The fact that $P_{Q_{i_k}}(\mathcal{A}\omega_{i_k}) \in Q_{i_k}$ implies

$$q(\mathcal{A}\omega_{i_k}) \leq \langle \vartheta_{i_k}, \mathcal{A}\omega_{i_k} - P_{Q_{i_k}}(\mathcal{A}\omega_{i_k}) \rangle, \quad (25)$$

where $\vartheta_{i_k} \in \partial q(\mathcal{A}\omega_{i_k})$. Then, we get

$$q(\mathcal{A}\omega_{i_k}) \leq \|\omega_{i_k}\| \|\mathcal{A}\omega_{i_k} - P_{Q_{i_k}}(\mathcal{A}\omega_{i_k})\| \rightarrow 0, k \rightarrow \infty.$$

Moreover, according to Eq. 25, we deduce

$$q(\mathcal{A}\omega^*) \leq \liminf_{k \rightarrow \infty} q(\mathcal{A}\omega_{i_k}) \leq 0.$$

Therefore, $\mathcal{A}\omega^* \in Q$. We can thus draw the conclusion that the sequence $\{\omega_{i_j}\} \rightarrow \Omega$.

4 Experimental results

In this section, we describe numerical simulations to demonstrate the applications of Yang’s algorithm [15], López’s algorithm [17], Sakurai and Iiduka’s algorithm [20], and the proposed algorithm (Algorithm 1) in signal processing and image recovery. The results of our simulations show that the proposed method has higher efficiency than the well-known methods in the literature. The experiments were carried out in the environment of Matlab2016 and the CPU is Intel(R) Core(TM) i5-8265U with @1.60GHz 1.80 GHz.

4.1 Signal processing

In the test, let original signal has m nonzero components, we choose $N = 4,096$, $M = 2048$, and $m = 128$ according to Eq. 1. The

mean value and variance of Gaussian noise are 0 and 10^{-4} , respectively. The initial point $\omega_1 = (1,1,\dots,1)^T$, $\omega_0 = (0,0,\dots,0)^T$, $\alpha_1 = 0.8$, $\alpha_2 = 0.9$, $\rho_i = 1.1$, $\theta_i = \frac{1}{i^2}$ and $r = m$. The mean squared error (MSE) can be chosen as the evaluation criterion, which is defined as:

$$MSE = \frac{1}{N} \|\omega^* - \omega\|^2,$$

where ω is the original signal, ω^* is the recovered signal. We set the stopping criteria $MSE \leq 10^{-5}$. Figure 1 shows the results of this experiment. These indicate that the number of iterations and CPU time required by our approach are the best of the four methods.

4.2 Image recovery

The value of each pixel in a grayscale image is in the range [0,255]. The image restoration can be described as the minimizer:

$$\min_{\bar{s} \in C} \|\mathcal{A}\bar{s} - y\|_2,$$

where $\|\cdot\|_2$ is the standard Euclidean norm, y is the observed image, \bar{s} is the approximation of the original image, and \mathcal{A} is a blurring operator. When a color image is processed, we divide it into three channels: red, green, and blue. Supposing the size of the image in each channel is $M \times N$, we have the formula for the MSE:

$$MSE = \frac{1}{MN} \sum_{i=0}^{M-1} \sum_{j=0}^{N-1} \|\bar{s}(i, j) - s(i, j)\|^2,$$

where \bar{s} and s are the restored and original images, respectively.

Seeking to illustrate the effects of image recovery, we use the signal-to-noise ratio (SNR) and peak SNR (PSNR), which are defined:

$$\text{SNR} := 20 \log_{10} \frac{\|\bar{s}\|_2}{\|s - \bar{s}\|_2}, \quad \text{PSNR} := 20 \log_{10} \frac{255}{\sqrt{\text{MSE}}}$$

In short, larger SNR and PSNR values indicate better restoration of the image. Figure 2 show the results of different color images recovery. Figure 3 shows a comparison of the SNR and PSNR values for images recovered using the four algorithms. The experimental results show that the proposed algorithm always has the largest SNR and PSNR values for different images, which clearly indicates that the proposed algorithm is more effective in recovery than other algorithms. We next applied our method to medical images. Figures 4, 5 show computed tomography (CT) images of a knee joint and a head, and Figure 6 shows a comparison of the SNR values resulting from recovery using each algorithm for these images. From Figure 6, it can be seen clearly that the SNR of our method (the red line) is significantly higher than other methods.

Figure 7 shows an original grayscale image. In Figure 8, we investigate the use of our method on this image with different sampling rates. In Figure 9, we show the image recovered by the four algorithms with different sampling rates. Figure 10 shows a comparison of the SNR values of these images. It can clearly be seen that the performance of our method is the best. Finally, it can clearly be seen that our method provides higher SNR and PSNR values than López's algorithm, Yang's algorithm, or Sakurai and Iiduka's algorithm.

5 Conclusion

In this article, we propose a new conjugate gradient method for signal recovery. The superiority of our method lies in its employment of the ideas of accelerated conjugate gradient methods with a new adaptive way of choosing the step size. Under some assumptions, the weak convergence of the designed method was established. As application demonstrations, we implemented our method to solve signal-processing and image-restoration problems. The results of our numerical simulations verify the effectiveness and superiority of the new approach. However, in the numerical experiments in this paper, we always assume that the noise is known. In the future work, we

References

- Zhang X, Wu H, Sun H, Ying W. Multireceiver SAS imagery based on monostatic conversion. *IEEE J Sel Top Appl Earth Obs Remote Sens* (2021) 14: 10835–53. doi:10.1109/jstars.2021.3121405
- Zhang X, Ying W, Yang P, Sun M. Parameter estimation of underwater impulsive noise with the Class B model. *IET Radar Sonar & Navigation* (2020) 14:1055–60. doi:10.1049/iet-rsn.2019.0477
- Li Y, Geng B, Jiao S. Dispersion entropy-based lempel–ziv complexity: A new metric for signal analysis. *Chaos Solitons Fractals* (2022) 161:112400. doi:10.1016/j.chaos.2022.112400
- Li Y, Tang B, Yi Y. A novel complexity-based mode feature representation for feature extraction of ship-radiated noise using VMD and slope entropy. *Appl Acoust* (2022) 196:108899. doi:10.1016/j.apacoust.2022.108899

will devote to signal and image recovery research without prior knowledge of noise by optimization method.

Data availability statement

The raw data supporting the conclusion of this article will be made available by the authors, without undue reservation.

Author contributions

PH and KL designed the work, wrote the manuscript, and managed communication among all the authors. PH and KL analyzed the data. All authors contributed to the article and approved the submitted version.

Funding

This project is supported by the Shandong Provincial Natural Science Foundation (Grant No. ZR2019MA022).

Acknowledgments

The authors would like to thank the reviewers and editors for their useful comments, which have helped to improve this article.

Conflict of interest

The authors declare that the research was conducted in the absence of any commercial or financial relationships that could be construed as a potential conflict of interest.

Publisher's note

All claims expressed in this article are solely those of the authors and do not necessarily represent those of their affiliated organizations, or those of the publisher, the editors and the reviewers. Any product that may be evaluated in this article, or claim that may be made by its manufacturer, is not guaranteed or endorsed by the publisher.

5. Li Y, Mu L, Gao P. Particle swarm optimization fractional slope entropy: A new time series complexity indicator for bearing fault diagnosis. *Fractal Fract* (2022) 6: 345. doi:10.3390/fractalfract6070345
6. Cai T, Xu G, Zhang J. On recovery of sparse signals via l_1 minimization. *IEEE Trans Inf Theor* (2009) 55:3388–97. doi:10.1109/tit.2009.2021377
7. Censor Y, Elfving T. A multiprojection algorithm using Bregman projections in a product space. *Numer Algorithms* (1994) 8:221–39. doi:10.1007/bf02142692
8. Xu H. Iterative methods for the split feasibility problem in infinite-dimensional Hilbert spaces. *Inverse Probl* (2010) 26:105018. doi:10.1088/0266-5611/26/10/105018
9. Moudafi A, Gibali A. l_1 - l_2 regularization of split feasibility problems. *Numer Algorithms* (2017) 78:739–57. doi:10.1007/s11075-017-0398-6
10. Bauschke H, Combettes P. A weak-to-strong convergence principle for Fejér-monotone methods in Hilbert spaces. *Mathematics OR* (2001) 26:248–64. doi:10.1287/moor.26.2.248.10558
11. Byrne C. Iterative oblique projection onto convex sets and the split feasibility problem. *Inverse Probl* (2002) 18:441–53. doi:10.1088/0266-5611/18/2/310
12. Byrne C. A unified treatment of some iterative algorithms in signal processing and image reconstruction. *Inverse Probl* (2004) 20:103–20. doi:10.1088/0266-5611/20/1/006
13. Yang Q. The relaxed CQ algorithm solving the split feasibility problem. *Inverse Probl* (2004) 20:1261–6. doi:10.1088/0266-5611/20/4/014
14. Wang F. Polyak's gradient method for split feasibility problem constrained by level sets. *Numer Algorithms* (2017) 77:925–38. doi:10.1007/s11075-017-0347-4
15. Yang Q. On variable-step relaxed projection algorithm for variational inequalities. *J Math Anal Appl* (2005) 302:166–79. doi:10.1016/j.jmaa.2004.07.048
16. Wang F. On the convergence of CQ algorithm with variable steps for the split equality problem. *Numer Algorithms* (2017) 74:927–35. doi:10.1007/s11075-016-0177-9
17. Lopez G, Martin-Marquez V, Wang F, Xu HK. Solving the split feasibility problem without prior knowledge of matrix norms. *Inverse Probl* (2012) 28:085004. doi:10.1088/0266-5611/28/8/085004
18. Qu B, Xiu N. A note on the CQ algorithm for the split feasibility problem. *Inverse Probl* (2005) 21:1655–65. doi:10.1088/0266-5611/21/5/009
19. Gibali A, Liu LW, Tang YC. Note on the modified relaxation CQ algorithm for the split feasibility problem. *Optim Lett* (2017) 12:817–30. doi:10.1007/s11590-017-1148-3
20. Kesornprom S, Pholasa N, Cholamjiak P. On the convergence analysis of the gradient-CQ algorithms for the split feasibility problem. *Numer Algorithms* (2020) 84:997–1017. doi:10.1007/s11075-019-00790-y
21. Nocedal J, Wright SJ. *Numerical optimization*. New York: Springer (2006).
22. Hiideaki I. Iterative algorithm for solving triple-hierarchical constrained optimization problem. *J Optim Theor Appl* (2011) 148:580–92. doi:10.1007/s10957-010-9769-z
23. Nocedal J. *Numerical optimization: Springer series in operations research and financial engineering*. New York: Springer (2006).
24. Sakurai K, Iiduka H. Acceleration of the Halpern algorithm to search for a fixed point of a nonexpansive mapping. *Fixed Point Theor Appl* (2014) 2014:202. doi:10.1186/1687-1812-2014-202
25. Dang Y, Gao Y. The strong convergence of a KM-CQ-like algorithm for a split feasibility problem. *Inverse Probl* (2011) 27:015007. doi:10.1088/0266-5611/27/1/015007
26. Suantai S, Pholasa N, Cholamjiak P. Relaxed CQ algorithms involving the inertial technique for multiple-sets split feasibility problems. *Rev Real Acad Cienc Exactas* (2019) 13:1081–99. doi:10.1007/s13398-018-0535-7
27. Wang F, Xu HK. Approximating curve and strong convergence of the CQ algorithm for the split feasibility problem. *J Inequal Appl* (2010) 2010:1–13. doi:10.1155/2010/102085
28. Xu H. Iterative methods for the split feasibility problem in infinite-dimensional Hilbert spaces. *Inverse Probl* (2010) 26:105018. doi:10.1088/0266-5611/26/10/105018
29. Zhao J, Zhang Y, Yang Q. Modified projection methods for the split feasibility problem and the multiple-sets split feasibility problem. *Appl Math Comput* (2012) 219:1644–53. doi:10.1016/j.amc.2012.08.005
30. Goebel K, Reich S. *Uniform convexity*. New York: Marcel Dekker (1984).